



 Cite this: *RSC Adv.*, 2020, 10, 4755

# Self-assembly of naturally occurring stigmasterol in liquids yielding a fibrillar network and gel†

 Braja Gopal Bag \* and Abir Chandan Barai

Stigmasterol, a naturally occurring 6-6-6-5 monohydroxy phytosterol, was extracted from the leaves of Indian medicinal plant *Roscoea purpurea*, commonly known as Kakoli. In continuation of our studies on the self-assembly properties of naturally occurring terpenoids, herein, we report the first self-assembly properties of this phytosterol in different organic liquids. The molecule self-assembled in organic liquids yielding supramolecular gels in most of the liquids studied *via* the formation of fibers and belt-like architectures of nano-to micrometer diameter. Characterization of the self-assemblies carried out by using scanning electron microscopy, transmission electron microscopy, atomic force microscopy, optical microscopy, FTIR and X-ray diffraction studies indicated fibrillar network and belt-like structures. A model for the self-assembly of stigmasterol has been proposed based on molecular modeling studies, X-ray diffraction data and FTIR studies. Rheology studies indicated that the gels were of high mechanical strength. Fluorophores such as rhodamine B, carboxy fluorescein including the anticancer drug doxorubicin could be loaded in the gels. Moreover, release of the loaded fluorophores including the drug has also been demonstrated from the gel phase into aqueous medium.

Received 10th December 2019

Accepted 21st January 2020

DOI: 10.1039/c9ra10376g

[rsc.li/rsc-advances](http://rsc.li/rsc-advances)

## 1. Introduction

Terpenoids including steroids are the major components of plant secondary metabolites. Steroids, like triterpenoids, are biosynthesized from oxido-squalene *via* a series of cation-olefin cyclizations and rearrangements.<sup>1</sup> Demethylations along with methyl migration and insertion produce steroids of diverse structures containing usually 24–29 carbons.<sup>2</sup> A complex mixture of various sterols is usually synthesized in higher plants, and is commonly referred to as phytosterols. Stigmasterol,  $\beta$ -sitosterol and campesterol are the major components among various phytosterols.<sup>3</sup> With their unique rigid 6-6-6-5 structural feature, sterols serve as indispensable components in cell membranes especially in higher plants and animals. The renewable nature of plant metabolites has made them highly significant in diversified areas of research in chemistry, biology and materials science because their utilizations in science and technology will aid in the development of a sustainable society.<sup>4–6</sup> Hierarchical self-assembly yielding supramolecular gels have created a great impact in research in advanced functional materials over the last two decades.<sup>7–14</sup> Such supramolecular gels have found applications in several fields<sup>15–18</sup> such as sensor devices,<sup>19</sup> thermo-chromic materials,<sup>20</sup> liquid crystals,<sup>21</sup> chemical catalysis,<sup>22</sup> electrically conductive scaffolds,<sup>23,24</sup>

templates for cell growth, inorganic structures,<sup>25</sup> cosmetics and food industries.<sup>7</sup> Chemical gels<sup>26–28</sup> include both synthetic polymeric gels as well as biopolymers which are based on covalent bonds and may involve cross-links. On the other hand, supramolecular physical gels<sup>29–33</sup> are typically made of low molecular weight compounds self-assembled *via* non-covalent interactions such as hydrogen-bonding, van der Waals, dipole–dipole, charge-transfer, aromatic–aromatic and coordination interactions. As a result, reversible gel-to-sol phase transitions occur in response to external stimuli such as heat, pH, ultra-sonication, *etc.*<sup>34,35</sup> Self-assembly of various types of amphiphiles such as proteins and peptides,<sup>36–38</sup> sugars,<sup>39,40</sup> fatty acids,<sup>41–43</sup> sphorolipids,<sup>44,45</sup> steroids,<sup>46,47</sup> *etc.* have been reported. Since the first report of the spontaneous self-assembly of a natural terpenoid betulinic acid yielding gels *via* the formation of fibrillar networks, self-assembly of several natural products have been reported,<sup>48</sup> even without functional transformation, during the last decade.<sup>49,50</sup> Stigmasterol, a natural 6-6-6-5 tetracyclic phytosterol, is present in plenty in higher plants. While investigating the chemical constituents of *Astava* plants,<sup>51</sup> we reported the first isolation of stigmasterol in the leaves of *Astava* plant *Roscoea purpurea*, commonly known as Kakoli.<sup>52</sup> Tremendous pharmacological effects like anti-osteoarthritic, hypoglycemic, anti-mutagenic, antioxidant, anti-inflammatory activity<sup>53</sup> including antigenotoxicity and anticancer activity<sup>54</sup> of stigmasterol have been reported. Just like terpenoids, stigmasterol is also a nano-sized molecule (1.73 nm) having both polar and non-polar regions (Fig. 1, 9 and 10). The structural characteristics of stigmasterol, having one polar

Department of Chemistry and Chemical Technology, Vidyasagar University, Midnapore 721102, West Bengal, India. E-mail: brajagb@gmail.com

† Electronic supplementary information (ESI) available: Energy minimized structures, details of thermodynamic parameters, FTIR, mode of self-assembly based on crystal packing, NMR spectra. See DOI: 10.1039/c9ra10376g



hydroxy group at one end and a large nonpolar lipophilic steroidal structure containing almost planar and rigid 6-6-6-5 skeleton and a flexible C10 branched chain, makes it an interesting amphiphile for the study of its self-assembly properties in different liquids (Fig. 1). Herein, we report the first self-assembly property of stigmasterol in different liquids yielding supramolecular gels *via* fibers of nano-to micro-meter dimensions. The morphology of the supramolecular gels of stigmasterol were characterized using several microscopic techniques like optical microscopy (OPM), scanning electron microscopy (SEM), transmission electron microscopy (TEM), atomic force microscopy (AFM). Based on molecular modeling studies, X-ray diffraction data and FTIR studies, a model for the self-assembly of stigmasterol has also been proposed. The gels were loaded with both cationic as well as anionic fluorophores including an anticancer drug. Release of the fluorophores from the loaded gels into aqueous medium was also demonstrated spectrophotometrically.

## 2. Results and discussion

### 2.1 Extraction, purification & isolation of stigmasterol

Even though isolation of stigmasterol has previously been reported from several plants,<sup>55,56</sup> first isolation of stigmasterol from the indian medicinal plant *Roscoeia purpurea* has been reported by us recently.<sup>52</sup> The molecule constitute a rigid tetracyclic backbone (6-6-6-5) with one secondary hydroxyl group at one end and one C10 branched hydrocarbon chain at the other end. Molecular modeling studies revealed that the molecule is 1.73 nm long (Fig. S1, ESI<sup>†</sup>) having an amphiphilic structure with a large lipophilic surface and a polar OH head group.

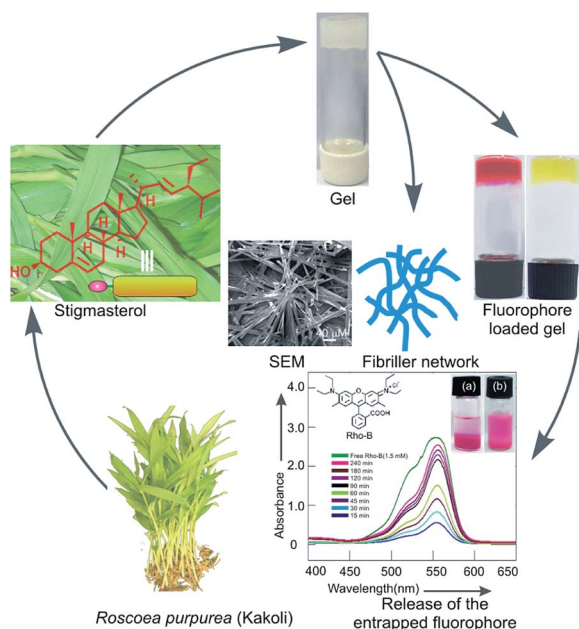


Fig. 1 Schematic representation of self-assembly of stigmasterol 1 in organic liquids forming supramolecular gel yielding fibrillar network.

Table 1 Self-assembly studies of stigmasterol

Entry	Solvent	State <sup>a</sup>	MGC	$T_{gel}^b$ (°C)
1	Nitrobenzene	G	42.40	30.3
2	<i>o</i> -Dichlorobenzene	G	56.53	29.9
3	<i>o</i> -Xylene	G	67.84	34.5
4	<i>m</i> -Xylene	VS	—	—
5	<i>p</i> -Xylene	VS	—	—
6	Cyclohexane	G	37.69	32.3
7	<i>n</i> -Hexane	G	17.00	31.5
8	<i>n</i> -Heptane	G	17.00	31.1
9	<i>n</i> -Octane	VS	—	—
10	DMF	G	42.40	30.3
11	DMSO	G	21.20	32.1
12	Ethanol	G	42.40	34.2
13	Methanol	G	24.23	33.1
14	Water	I	—	—

<sup>a</sup> G = gel, VS = viscous suspension, I = insoluble, minimum gelator concentration MGC are given in mM unit. <sup>b</sup>  $T_{gel}$  = gel to sol transition temperatures.

### 2.2 Study of self-assembly properties

Self-assembly studies of stigmasterol were carried out in both polar as well as non-polar organic liquids. Typically for such studies, a certain amount of stigmasterol (usually 3–5 mg) was dissolved in the liquid contained in a vial under hot condition with magnetic stirring. Then the solution was kept at room temperature (25 °C) and observed visually. When the material did not flow by turning the vial upside down, we called it a gel. Self-assembly of stigmasterol was carried out in 13 organic liquids. Among the 13 neat organic liquids tested, stigmasterol self-assembled in all the liquids in the concentration range of 1–6% w/v (17–68 mM) forming opaque gels in 10 neat liquids such as dimethyl sulfoxide (DMSO), nitro benzene, cyclohexane, *n*-hexane and *n*-heptane *etc.* (Table 1). In non-polar liquids such as *n*-hexane, *n*-heptane and cyclohexane, gels were formed almost instantaneously (within 1–5 min). In the other liquids, gels were obtained in 30 min to 1 h. The minimum gelator concentration (MGC) values for the gels obtained in different liquids were in the concentration ranges of 17–68 mM. Stigmasterol was found to be the best gelator for *n*-hexane and *n*-heptane with 17 mM being the MGC values for both the liquids.

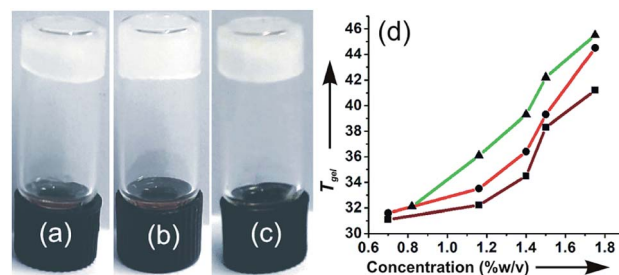


Fig. 2 A gel of stigmasterol in (a) DMSO (b) *n*-hexane and (c) *n*-heptane; (d) plots of  $T_{gel}$  versus concentration for 1 in DMSO (-▲-); *n*-hexane (-●-); *n*-heptane (-■-).



Table 2 Thermodynamic parameters ( $\Delta H^\circ$ ,  $\Delta S^\circ$ ,  $\Delta G^\circ$ ) for gel to sol transition of gels of stigmasterol **1** in different liquids at 298 K

Liquid	$\Delta H^\circ/\text{kJ mol}^{-1}$	$\Delta S^\circ/\text{J mol}^{-1} \text{K}^{-1}$	$\Delta G^\circ/\text{kJ mol}^{-1}$
<i>n</i> -Hexane	24.01	49.33	9.317
<i>n</i> -Heptane	31.30	73.24	9.473
DMSO	28.73	63.79	9.730

Viscous suspensions were obtained in *m*-xylene, *p*-xylene and *n*-octane. All the gels were thermally reversible with their sol phases. The thermo-reversibility of the gels was confirmed by repeatedly heating the gel to melt and then allowing resulting solution to cool to regenerate the gel. This thermo-reversibility of the gels allowed us to plot the gel to sol transition temperature  $T_{\text{gel}}$  vs. % of gelator concentration. Increase in the concentration of the gelator, the  $T_{\text{gel}}$  values increased which indicated the stronger intermolecular interactions at higher concentrations. The  $T_{\text{gel}}$  value for *n*-hexane and *n*-heptane gels at its MGC (17 mM) was 31.5 and 31.1 °C and increased to 44.5 and 41.2 °C respectively at 42.40 mM concentration (Fig. 2). Similarly, the  $T_{\text{gel}}$  value of the DMSO gel at MGC (21.20 mM) was 32.1 °C and increased to 45.5 °C (Fig. 2d and S2, ESI<sup>†</sup>) at 42.40 mM concentration. The various thermodynamic parameters ( $\Delta H^\circ$ ,  $\Delta S^\circ$  and  $\Delta G^\circ$ ) at 298 K were calculated from the plot of  $\ln K$  vs.  $1/T_{\text{gel}}$  (Fig. S2, ESI<sup>†</sup>). The free energy changes (Table 2) observed during gel to sol transformations in all the cases were in the range of (+) 9.32 to (+) 9.73  $\text{kJ mol}^{-1}$  which is indicative of stability of the gels. It is also worth noting that even though the  $\Delta H^\circ$  values for the three liquids were different, the  $\Delta G^\circ$  values were very close due to compensation by the  $\Delta S^\circ$  values.

### 2.3 Morphological characteristics of the self-assemblies

Morphology of the self-assemblies were studied by polarized optical microscope (POM), atomic force microscopy (AFM), scanning electron microscopy (SEM) and FTIR studies.

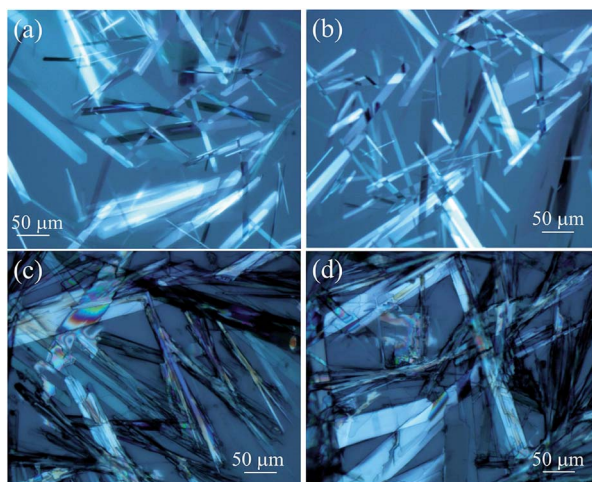


Fig. 3 Polarizing optical microscopy images of **1** in (a) and (b) *m*-xylene (67.87 mM) (c) and (d) *o*-xylene (67.87 mM).

**2.3.1 Optical microscopic images.** The morphology of the gels were studied by optical microscopy. The OPM images showed different microstructures of the gels in different liquids. Sheet like structures with optical birefringence of 2–3 micrometre cross-sections and up to 100 micrometre lengths were observed in a gel of stigmasterol in nitrobenzene, *o*-xylene, *m*-xylene and DMSO under polarized light (Fig. 3). Fibrillar networks having nano to micrometre lengths were observed in the gels of stigmasterol in cyclohexane, *n*-hexane and *n*-heptane (Fig. 4).

**2.3.2 Scanning electron microscopic studies.** The self-assemblies of **1** prepared from the colloidal suspensions in cyclohexane and *n*-heptane were studied by scanning electron microscopy. Densely packed and entangled fibrillar networks were observed (Fig. 5). Belt-like self-assemblies were also obtained in *o*-dichloro benzene (26.65 mM) (Fig. S3, ESI<sup>†</sup>). Bundles of fibers with diameters 0.407–2.21  $\mu\text{m}$  were observed in cyclohexane. As the molecule is 1.73 nm long (Fig. S1, ESI<sup>†</sup>), several molecules are present in the cross-section of the fibers. Although the fibrillar network of micrometer diameter was obtained in all the dried self-assemblies studied, their shapes were not identical probably due to sensitivity of the solute towards the liquid. Fibrillar self-assemblies from different type of surfactant and peptide have been reported.<sup>57,58</sup> But such fibrillar self-assemblies from naturally occurring phytosterols are rare.

**2.3.3 HRTEM studies.** HRTEM studies carried out with the dried self-assemblies of **1** prepared from the colloidal suspensions in *n*-heptane (2.5 mM) indicated the formation of belt-like networks having nano-to micro-meter cross-sections and micrometer lengths (Fig. 6). All these observations support the results obtained by SEM and optical microscopy studies (discussed earlier).

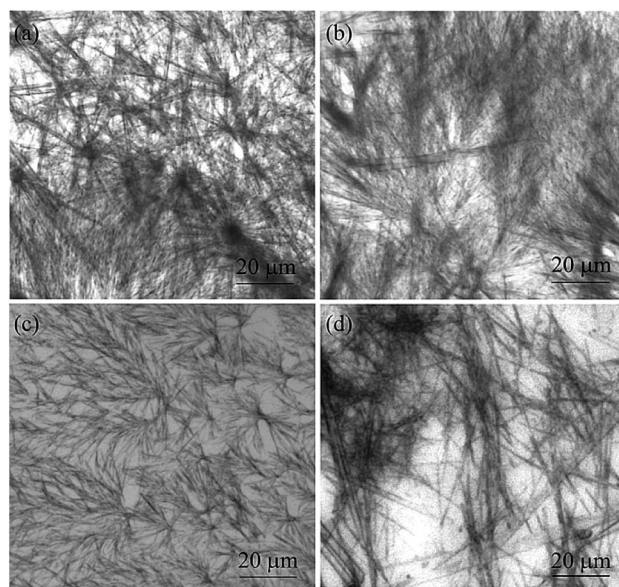


Fig. 4 Optical microscopy images of **1** in (a) and (b) *n*-hexane (17 mM) (c) *n*-heptane (17 mM) and (d) cyclohexane (37.69 mM).



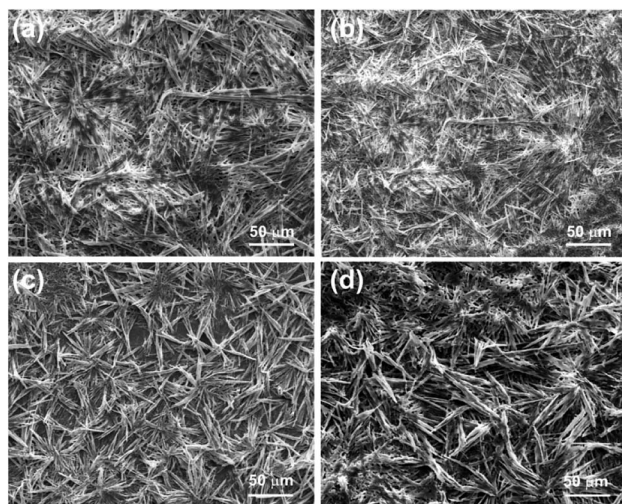


Fig. 5 (a–d) Scanning electron micrographs of the dried self-assemblies of stigmasterol prepared from dilute solution in *n*-heptane (25.92 mM).

**2.3.4 Atomic force microscopic images.** Atomic force microscopy of a dried sample prepared from the solution of **1** (6.08 mM) in *n*-hexane and *n*-heptanes indicated the formation of self-assemblies of 400 nm to 900 nm cross-sections and 3–6 micrometre lengths (Fig. 7). All these observations support the results obtained by TEM, SEM and optical microscopy studies (discussed earlier).

**2.3.5 Rheology study of gel.** For studying the mechanical properties of gel, rheology experiment was carried out using CP 25 cone plate at 25 °C (Fig. 8a). The storage modulus ( $G'$ ) and loss modulus ( $G''$ ) were measured in amplitude sweep experiment (Fig. 8a). For a gel of stigmasterol in DMSO (49 mM), the storage modulus  $G'$  and the loss modulus  $G''$  moved almost

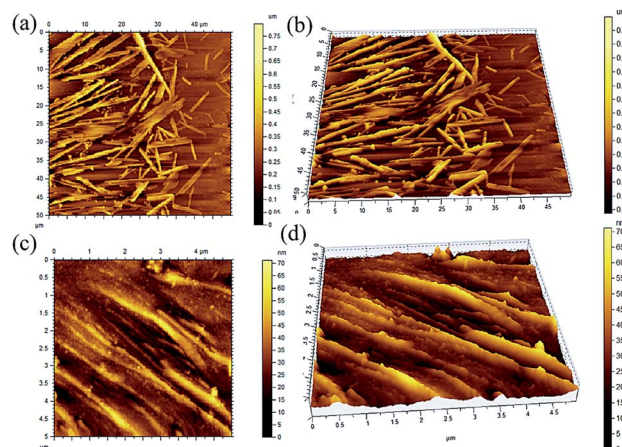


Fig. 7 AFM images (a and c) 2D, (b and d) 3D of the self-assemblies of stigmasterol in (a and b) *n*-heptane (6.057 mM) (c and d) cyclohexane (6.06 mM).

parallelly during a long range until a cross over point was reached. The storage modulus ( $G'$ ) for the gel is of the order of  $5 \times 10^3$  Pa indicating its high mechanical strength.<sup>68</sup>

**2.3.6 FTIR, X-ray diffraction and molecular modelling studies.** Infrared spectra of self-assembled stigmasterol were performed in different liquids in their gel state and the change in the 'O–H' stretching vibration were compared with that in the dried powder sample of the compound. An overlay of the FTIR spectra clearly indicated the shifts of the 'O–H' stretching frequency in the gels in cyclohexane, *n*-hexane and

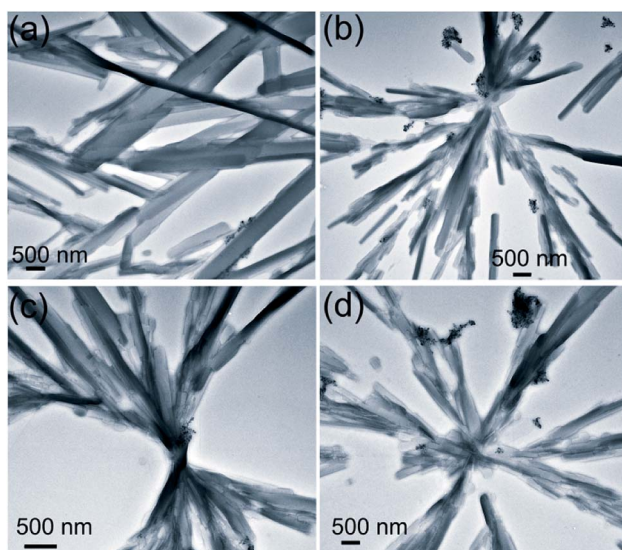


Fig. 6 HRTEM (unstained) of self-assembled stigmasterol in *n*-heptane (2.5 mM).

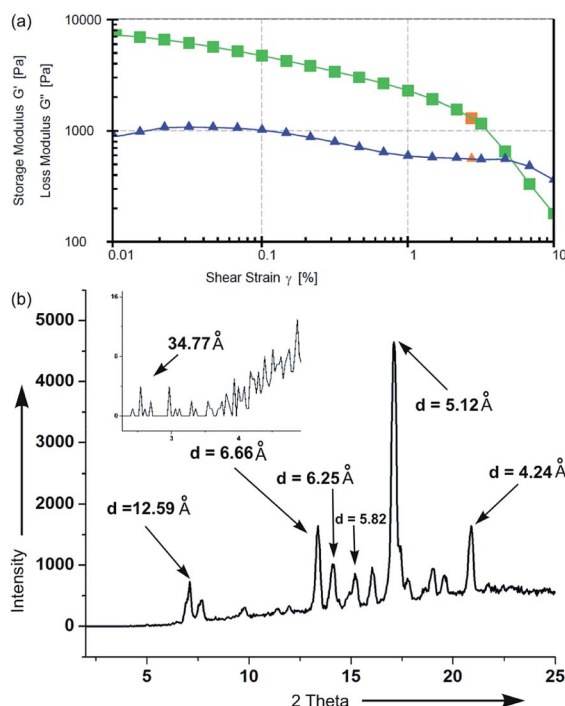


Fig. 8 (a) Rheology of gel of **1** in DMSO (49 mM). (b) X-ray diffraction study of xerogel of **1** in *n*-hexane.



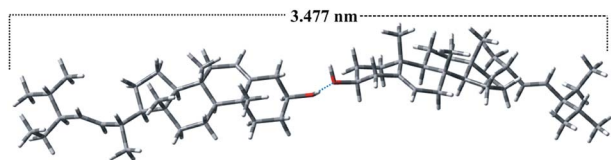


Fig. 9 Energy-minimized structure of stigmasterol: the length of the molecule is 1.73 nm. Two molecules are formed dimeric structure by H-bonding and the length of the dimer is 3.47 nm.

nitrobenzene (Fig. S4, ESI†). For example, the stretching frequency of the 'O-H' group in the neat powder appeared at  $3437\text{ cm}^{-1}$ , whereas the stretching frequency of 'O-H' group in the self-assemblies prepared from cyclohexane, *n*-hexane, and nitrobenzene appeared at  $3342\text{ cm}^{-1}$ ,  $3343\text{ cm}^{-1}$  and  $3345\text{ cm}^{-1}$  respectively. It was clearly observed that the stretching frequency of 'O-H' in cyclohexane, *n*-hexane and nitrobenzene shifted to the lower frequency (red shift) because of the weakening of the -O-H bond. Broadening of the -O-H stretching bands is due to the formation of hydrogen bonds.<sup>59,60</sup> The shifting in the -O-H stretching frequencies clearly indicated that the self-assembly is driven by the intermolecular H-bonding among the molecules.

To throw light on the mode of self-assembly of stigmasterol molecules, low angle X-ray powder diffraction (XRD) experiments and molecular modelling studies using Pmodel 9.2 and GaussView 5.0 software were carried out. The powder diffraction

peaks were compared with the simulated peaks obtained from the reported crystal structure of stigmasterol hemihydrate.<sup>61,62</sup> The X-ray diffraction spectra of xerogels of stigmasterol in cyclohexane (Fig. 8) show diffraction peaks with a *d*-spacing of 34.77 Å. Interestingly, the optimized length of hydrogen bonded dimeric stigmasterol is 34.77 Å (Fig. 9), that exactly matches with the above *d*-spacing data. This supports the presence of H-bond in the self-assemblies.<sup>63,64</sup> The computer generated X-ray powder diffraction peaks obtained from the X-ray crystal structure (Fig. S5, ESI†) had several common peaks with the diffraction peaks obtained for the xero-gel (Fig. 8b) though the intensities were different. This indicated that even though the morphs of stigmasterol in the crystal and in the xero-gel were not identical, certain percentage of ordered morphology are present even in the xero-gel.

Both energy minimized structure and the crystal structure of stigmasterol supports the planar structure. Based on the energy minimized H-bonded dimeric structure of stigmasterol and the crystal structure, various modes of assembly of the steroids has been proposed (Fig. 10 and S6–S10, ESI†). The  $\alpha$  and  $\beta$  faces of the steroid are not identical. This non-identical nature of the surfaces gives rise to three distinct modes of parallel stacked arrangements such as  $\alpha\alpha$ ,  $\alpha\beta$ ,  $\beta\beta$ . Thorough inspection of the crystal structure of stigmasterol revealed two distinct modes of parallel stacked arrangements namely  $\alpha\alpha$  and  $\beta\beta$ . Assuming that identical face to face parallel stacked arrangements are also present in self-assembled stigmasterol, two modes of face to face dimeric structures I and II (Fig. 10, S6 and S7, ESI†) are

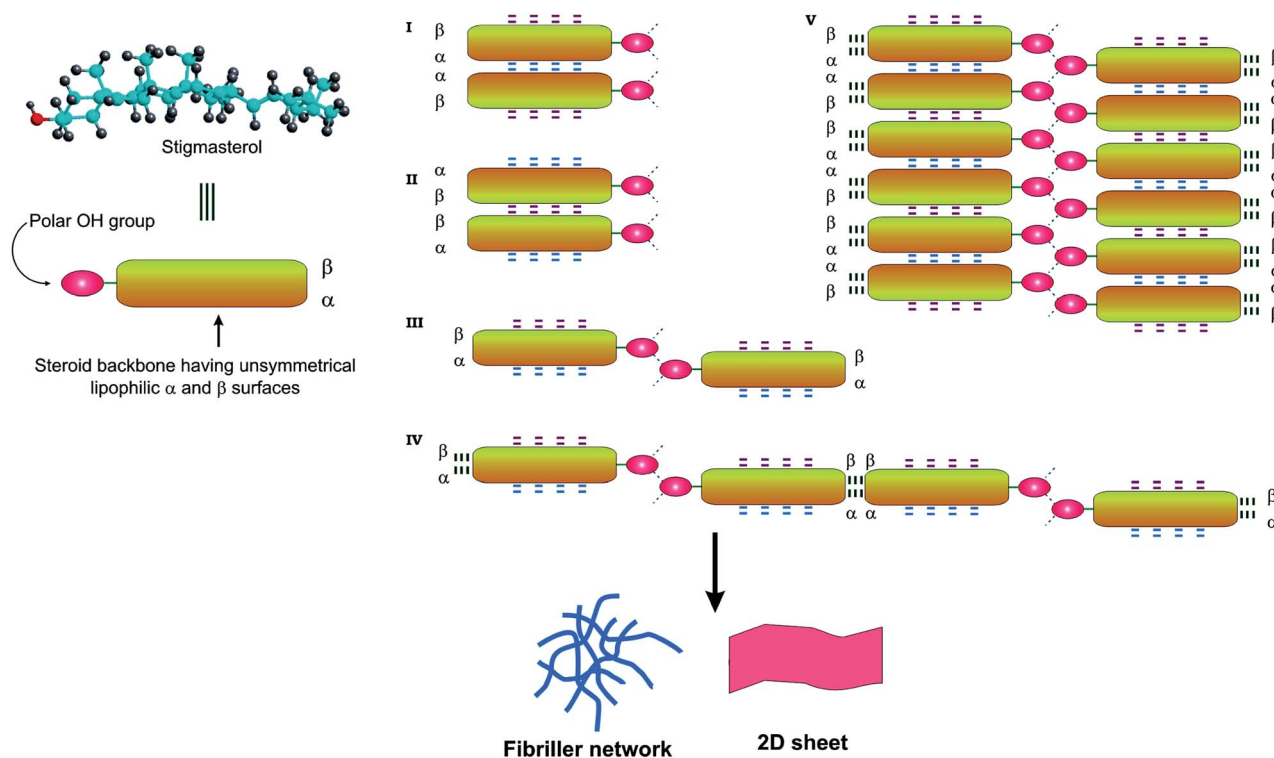


Fig. 10 Schematic representation of various modes of self-assembly of stigmasterol. The OH groups can take part in H-bonding and the lipophilic surface of steroid can take part in van der Waals interaction. The  $\alpha$  and  $\beta$  face of the steroid leads to two types of assembly formation of the type I–V.



proposed. The H-bonded dimeric structure III (Fig. 10 and S8, ESI†) can be extended to form 1D fibrillar network, bilayer assembly and 2D sheet structure (IV and V in Fig. 10, S9 and S10, ESI†). Analysis of crystal packing of stigmasterol reveals that both in  $\alpha\alpha$  and  $\beta\beta$  face-to-face stacked arrangements, the steroid surfaces are within van der Waals contact distance supporting the role of van der Waals interaction in the self-assemblies.<sup>65</sup>

### 3. Utilization of gel in entrapment and subsequent release of fluorophores including anticancer drug

Fibrillar self-assemblies of the solute molecules present inside the supramolecular gel possess a high surface area.<sup>66,67</sup> Moreover, the gels possess a porous microstructure filled with the

liquid.<sup>50,68</sup> Whether the supramolecular gels of **1** obtained in different liquids are capable of entrapping guest molecules inside, we examined the entrapment of the cationic fluorophore rhodamine B (Rho-B) and an anionic fluorophore 5,6 carboxy-fluorescein (CF). Interestingly, when gelation studies of **1** in different liquids were carried out in the presence of the fluorophores as guests, formation of coloured gels were observed (Fig. 11(II and V)). For example, when a hot solution of stigmasterol in DMSO (225  $\mu$ L, 40 mM) was mixed with a solution of Rho-B in DMSO (75  $\mu$ L, 6 mM) and the mixture was heated to obtain a colored solution and the resulting mixture was allowed to cool at room temperature, the Rho-B entrapped reddish gel was formed instantly (Fig. 11(II)). In an identical method, CF loaded yellowish gel was also obtained in DMSO (Fig. 11(V)). Intense fluorescence of the fluorophore loaded gels were obtained in both the cases when observed under 366 nm UV light

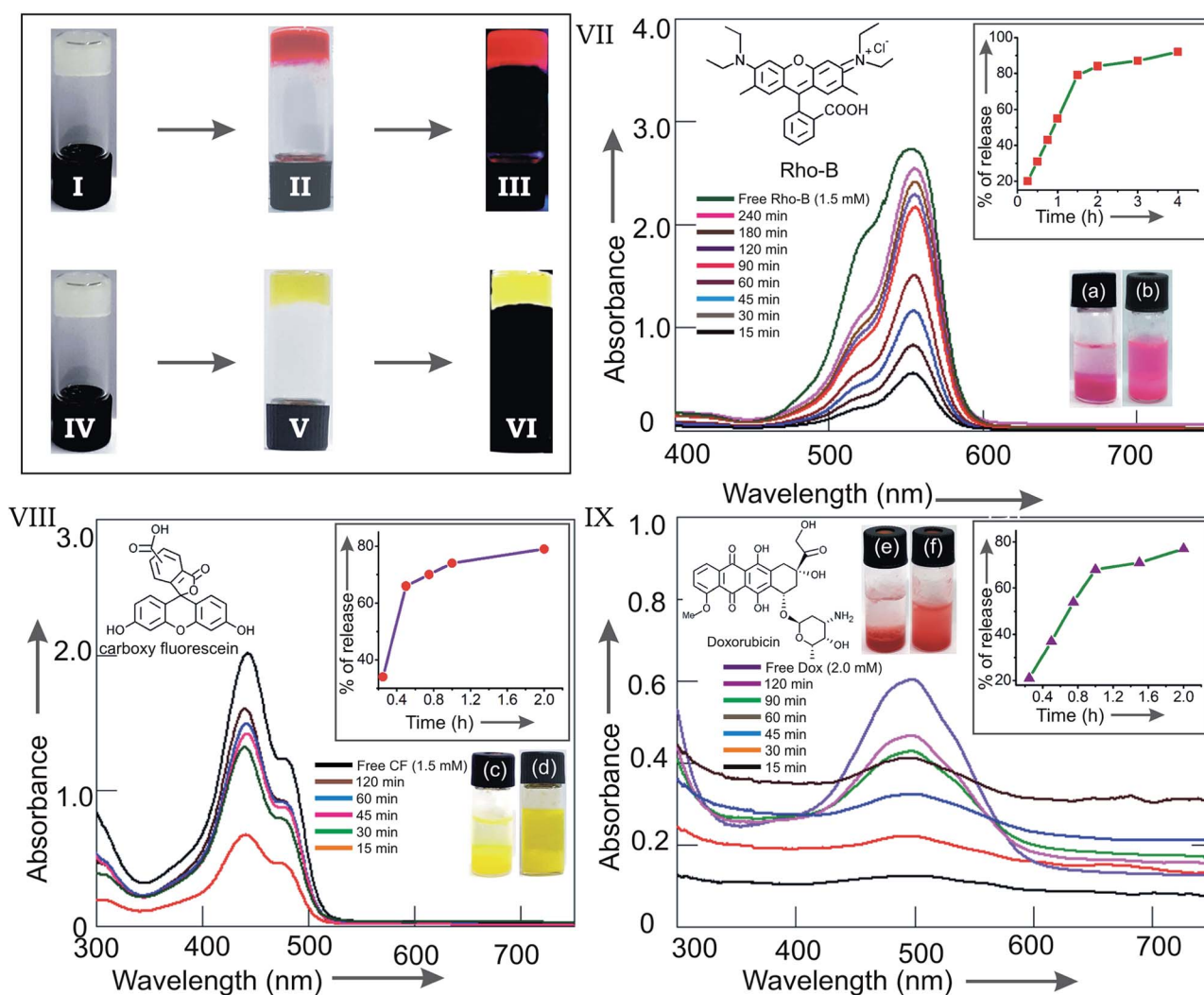


Fig. 11 Inverted vials containing gels of **1** in DMSO (I and IV). Rho-B loaded gel of **1** in DMSO (II under normal light and III under 366 nm UV light). CF loaded gel of **1** in DMSO (V under normal light and VI under 366 nm UV light). Release of the fluorophores Rho-B (VII), CF (VIII) and the anticancer drug Doxorubicin (IX) from Rho-B (1.5 mM), CF (1.5 mM) and Doxorubicin (2.0 mM) loaded gels of stigmasterol (40 mM) in DMSO (300  $\mu$ L) respectively into aqueous media (900  $\mu$ L): overlay of the UV-visible spectra of released Rho-B (VII), CF (VIII) and DOX (IX) into aqueous media at various time intervals. Inset in VII, VIII and IX are the plots of % of release of fluorophore/drug vs. time for the respective experiments.



(Fig. 11(III and VI)) confirming the loading of the fluorophores inside the gel network.

To find out whether the gel-entrapped fluorophores can be released, we carried out the release studies with the Rho-B and CF loaded gels into water. Rho-B (1.5 mM) loaded gel of stigmasterol in DMSO (300  $\mu\text{L}$ , 40 mM) contained in a vial was kept in equilibrium with water (900  $\mu\text{L}$ ). The release of Rho-B was monitored by UV-visible spectroscopy after collecting the aliquots carefully from the top of the vial at various time intervals. The aliquots were returned back to the vial carefully after each absorption measurement. Significant release of Rho-B (92%) from the DMSO gel into aqueous medium was observed after 4 h (Fig. 11(VII)). To investigate whether the anionic fluorophore CF can also be released from the CF loaded gel, we carried out the release study of CF into water following the above method. A significant release of CF (79%) from the CF loaded DMSO gel into the aqueous medium was observed after 2 h (Fig. 11(VIII)). A plot of the percentage release of fluorophore vs. time indicated that initially the rate of release were very fast and then it reached saturation after approximately 2 h of equilibration with water (Fig. 11 inset in VII and VIII). Assuming a non-steady state diffusion model (see ESI Page S13†) for the release of fluorophore,<sup>68</sup> the diffusion coefficients for Rho-B and CF were calculated to be  $2.88 \times 10^{-10} \text{ m}^2 \text{ s}^{-1}$  and  $4.25 \times 10^{-10} \text{ m}^2 \text{ s}^{-1}$  respectively. These values were comparable to the values reported by others.

### 3.1 Release of the anticancer drug doxorubicin

The success in the entrapment and release experiments of cationic and anionic fluorophores inspired us to examine the entrapment and release of the anticancer drug doxorubicin.<sup>69</sup> When a doxorubicin (2 mM) loaded gel of **1** (40 mM) in DMSO (300  $\mu\text{L}$ ) was kept in equilibrium with water and the release of the drug molecule was monitored by UV-visible spectroscopy at various time intervals, 77% release of the entrapped doxorubicin was observed (Fig. 11(IX)) in 2 h, making it useful for potential drug delivery applications. A plot of the percentage release of doxorubicin vs. time indicated a very fast release in the beginning and then it reached saturation after approximately 90 min (inset in Fig. 11(IX)). The diffusion coefficient for doxorubicin was calculated to be  $4.04 \times 10^{-10} \text{ m}^2 \text{ s}^{-1}$  (see ESI Page S13†).<sup>68</sup>

## 4. Conclusions

Self-assembly of stigmasterol isolated from the medicinal plant *Roscoea purpurea* in liquids has been reported. According to our knowledge, this is the first report of self-assembly of stigmasterol in liquids. The molecule self-assembled in all the organic liquids yielding nano-to micrometer diameter fibers and belt-like architecture. Characterization of the self-assemblies were carried out by optical, electron and atomic force microscopic techniques and X-ray diffraction studies. Thermo-reversible supramolecular gels were formed in most of the liquids studied. The supramolecular gels could entrap fluorophores such as rhodamine B, carboxy fluorescein including the

anticancer drug doxorubicin. Additionally, release of the loaded fluorophores including the anticancer drug from the gel into aqueous medium was also demonstrated. Biosynthetically sterols being of triterpenoid origin, stigmasterol joins the larger family of terpenoid based natural products yielding self-assemblies and gels in liquids.

## 5. Experimental

### 5.1 Materials

Stigmasterol was isolated from the dried and powdered leaves of Kakoli (*Roscoea purpurea*) in 0.14% yield as a white solid.<sup>52</sup>

### 5.2 Preparation of self-assemblies/gel

Compound **1** (1–5 mg) of contained in a vial (1 cm id) was heated with a liquid with continuous magnetic stirring over a hot plate until a clear solution was obtained. The solution was then allowed to cool at room temperature (24–25 °C) and observed. When the material did not flow as observed by turning the vial upside down, we called it a gel. The morphology of the samples were observed initially by optical microscopy and then by the techniques described before.

## Conflicts of interest

The authors declare no conflict of interest

## Acknowledgements

BGB thanks India Srilanka project (DST/INT/SL/P25/2016), Science and Engineering Research Board (SERB), India (ref. EMR/2017/000069), UGC-SAP and DST-FIST New Delhi and Vidyasagar University for financial support and infrastructural facilities. ACB acknowledges UGC for a research fellowship.

## Notes and references

- 1 K. Ohyamaa, M. Suzukia, J. Kikuchi, K. Saitoa and T. Muranaka, *Proc. Natl. Acad. Sci. U. S. A.*, 2009, **106**, 725.
- 2 E. J. Corey, S. P. T. Matsuda and B. Bartel, *Proc. Natl. Acad. Sci. U. S. A.*, 1993, **90**, 11628.
- 3 P. Benveniste, *Annu. Rev. Plant Biol.*, 2004, **55**, 429.
- 4 B. Kamm, *Angew. Chem., Int. Ed.*, 2007, **46**, 5056.
- 5 A. Gandini, *Green Chem.*, 2011, **13**, 1061.
- 6 B. G. Bag, A. C. Barai, S. N. Hasan, S. K. Panja, S. Ghorai and S. Patra, *Pure Appl. Chem.*, 2019, DOI: 10.1515/pac-2019-0812.
- 7 M. George and R. G. Weiss, *Acc. Chem. Res.*, 2006, **39**, 489–497.
- 8 B. G. Bag and R. Majumdar, *Chem. Rec.*, 2017, **17**, 841.
- 9 E. Carretti, M. Bonini, L. Dei, B. H. Berrie, L. V. Angelova, P. Baglioni and R. G. Weiss, *Acc. Chem. Res.*, 2010, **43**, 751–760.
- 10 S. Bhattacharya and S. K. Samanta, *Chem. Rev.*, 2016, **116**, 11967.
- 11 K. Hanabusa, *Springer Ser. Mater. Sci.*, 2004, **78**, 118.



- 12 *Molecular Gels: Materials with Self-Assembled Fibrillar Networks*, ed. R. G. Weiss and P. Terech, Springer, Dordrecht, 2006.
- 13 M. George and R. G. Weiss, *Chem. Mater.*, 2003, **15**, 2879–2888.
- 14 M. de Loos, B. L. Feringa and J. H. van Esch, *Eur. J. Org. Chem.*, 2005, 3615.
- 15 A. Vintiloui and J.-C. Leroux, *J. Controlled Release*, 2008, **125**, 179.
- 16 J. H. Jung and S. Shinkai, *Top. Curr. Chem.*, 2004, **248**, 223.
- 17 R. V. Ulijn and A. M. Smith, *Chem. Soc. Rev.*, 2008, **37**, 664.
- 18 M. O. M. Piepenbrock, G. O. Lloyd, N. Clarke and J. W. Steed, *Chem. Rev.*, 2010, **110**, 1960.
- 19 S. Li, V. T. John, G. C. Irvin, S. H. Bachakonda, G. L. McPherson and C. J. O'Connor, *J. Appl. Phys.*, 1999, **85**, 5965.
- 20 B. G. Bag, G. C. Maity and S. K. Dinda, *Org. Lett.*, 2006, **8**, 5457.
- 21 T. Kato, *Science*, 2002, **295**, 2414.
- 22 D. D. Díaz, D. Kühbeck and R. J. Koopmans, *Chem. Soc. Rev.*, 2011, **40**, 427.
- 23 J. Puigmarti-Luis, V. Laukhin, A. P. del Pino, J. Vidal-Gancedo, C. Rovira, E. Laukhina and D. B. Amabilino, *Angew. Chem., Int. Ed.*, 2007, **46**, 238.
- 24 W. Kubo, S. Kambe, S. Nakade, T. Kitamura, K. Hanabusa, Y. Wada and S. Yanagida, *J. Phys. Chem. B*, 2003, **107**, 4374.
- 25 C. Sanchez and M. Llusar, *Chem. Mater.*, 2008, **20**, 782.
- 26 T. Tanaka, *Sci. Am.*, 1981, **244**, 110.
- 27 *Polymer Gels, Fundamentals and Biomedical Applications*, ed. D. DeRossi, Y. Kajiwara, Y. Osada and A. Yamauchi, Plenum Press, New York, 1991.
- 28 S.-K. Ahn, R. M. Kasi, S.-C. Kim, N. Sharma and Y. Zhou, *Soft Matter*, 2008, **4**, 1151.
- 29 L. A. Estroff and A. D. Hamilton, *Chem. Rev.*, 2004, **104**, 1201.
- 30 P. Xie and R. Zhang, *J. Mater. Chem.*, 2005, **15**, 2529.
- 31 A. Ajayaghosh, V. K. Praveen and C. Vijayakumar, *Chem. Soc. Rev.*, 2008, **37**, 109.
- 32 *Molecular Gels: Materials with Self-Assembled Fibrillar Networks*, ed. R. G. Weiss and P. Terech, Springer, 2006.
- 33 D. K. Smith, *Chem. Commun.*, 2006, 34–44.
- 34 F. Ilmain, T. Tanaka and E. Kokufuta, *Nature*, 1991, **349**, 400.
- 35 *Polymer Gels and Networks*, ed. Y. Osada and A. R. Khokhlov, Marcel Dekker, New York, 2002.
- 36 Y. Jang and J. A. Champion, *Acc. Chem. Res.*, 2016, **49**, 2188–2198.
- 37 D. Das, T. Kar and P. K. Das, *Soft Matter*, 2012, **8**, 2348.
- 38 P. Koley and A. Pramanik, *Adv. Funct. Mater.*, 2011, **21**, 4126.
- 39 S. Datta and S. Bhattacharya, *Chem. Soc. Rev.*, 2015, **44**, 5596.
- 40 H. Kobayashi, A. Friggeri, K. Koumoto, M. Amaike, S. Shinkai and D. N. Reinhoudt, *Org. Lett.*, 2002, **4**, 1423.
- 41 M. Delample, F. Jerome, J. Barrault and J. P. Douliez, *Green Chem.*, 2011, **13**, 64.
- 42 B. Novales, L. Navailles, M. Axelos, F. Nallet and J. P. Douliez, *Langmuir*, 2008, **24**, 62–68.
- 43 J. P. Douliez, *J. Am. Chem. Soc.*, 2005, **127**, 15694.
- 44 N. Baccile, N. Nassif, L. Malfatti, I. N. A. VanBogaert, W. Soetaert, G. Pehau-Arnaudet and F. Babonneau, *Green Chem.*, 2010, **12**, 1564.
- 45 S. Zhou, C. Xu, J. Wang, W. Gao, R. Khverdiyeva, V. Shah and R. Gross, *Langmuir*, 2004, **20**, 7926.
- 46 E. Virtanen and E. Kolehmainen, *Eur. J. Org. Chem.*, 2004, **16**, 3385.
- 47 N. He, K. Zhi, X. Yang, H. Zhao, H. Zhang, J. Wang and Z. Wang, *New J. Chem.*, 2018, **42**, 14170.
- 48 B. G. Bag and S. S. Dash, *Nanoscale*, 2011, **3**, 4564.
- 49 B. G. Bag, S. Das, S. N. Hasan, A. C. Barai, S. Ghorai, S. K. Panja and C. Garai Santra, *Prayogik Rasayan*, 2018, **2**, 1–23.
- 50 B. G. Bag, S. N. Hasan, P. Pongpamorn and N. Thasana, *ChemistrySelect*, 2017, **2**, 6650–6657.
- 51 R. Marde and R. K. Mishra, *Int. J. Unani. Integ. Med.*, 2019, **3**, 08–12.
- 52 A. C. Barai and B. G. Bag, *Prayogik Rasayan*, 2019, **3**, 5.
- 53 N. Kaur, J. Chaudhary, A. Jain and L. Kishore, *Int. J. Pharm. Sci. Res.*, 2011, **2**, 2259–2265.
- 54 H. Ali, S. Dixit, D. Ali, S. M. Alqahtani, S. Alkahtani and S. Alarifi, *Drug Des. Dev. Ther.*, 2015, **9**, 2793–2800.
- 55 M. A. Zeb, S. U. Khan, T. U. Rahman, M. Sajid and S. Seloni, *Pharm. Pharmacol. Int. J.*, 2017, **5**, 204–207.
- 56 P. S. Jain and S. B. Bari, *Asian J. Plant Sci.*, 2010, **9**, 163–167.
- 57 D. Wang and J. Hao, *Langmuir*, 2011, **27**, 1713–1717.
- 58 J. Schiller, J. V. A. Requena, E. M. López, R. P. Herrera, J. Casanovas, C. Alemánd and D. Díaz, *Soft Matter*, 2016, **12**, 4361.
- 59 A. Ajayaghosh and S. J. George, *J. Am. Chem. Soc.*, 2001, **123**, 5148–5149.
- 60 J. J. Dannenberg, *J. Am. Chem. Soc.*, 1998, **120**, 5604.
- 61 G. A. Benavides, F. R. Fronczek and N. H. Fischer, *Acta Crystallogr.*, 2002, **58**, o131–o132.
- 62 Mercury 4.2.0 (Build 257471), <http://www.ccdc.cam.ac.uk/mercury/>.
- 63 J. Wu, T. Yi, T. Shu, M. Yu, Z. Zhou, M. Xu, Y. Zhou, H. Zhang, J. Han and F. Li, *Angew. Chem., Int. Ed.*, 2008, **47**, 1063–1067.
- 64 P. Xue, R. Lu, Y. Huang, M. Jin, C. Tan, C. Bao, Z. Wang and Y. Zhao, *Langmuir*, 2004, **20**, 6470–6475.
- 65 M. Zinic, F. Vögtle and F. Fages, *Top. Curr. Chem.*, 2005, **256**, 39–76.
- 66 J. Mayr, C. Saldías and D. D. Díaz, *Chem. Soc. Rev.*, 2018, **47**, 1484.
- 67 L. Gu, A. Faig, D. Abdelhamid and K. Urich, *Acc. Chem. Res.*, 2014, **47**, 2867–2877.
- 68 A. Baral, S. Roy, A. Dehsorkhi, I. W. Hamley, S. Mohapatra, S. Ghosh and A. Banerjee, *Langmuir*, 2014, **30**, 929–936.
- 69 K. Basu, A. Baral, S. Basak, A. Dehsorkhi, J. Nanda, D. Bhunia, S. Ghosh, V. Castelletto, I. W. Hamley and A. Banerjee, *Chem. Commun.*, 2016, **52**, 5045.

